Research Square

Preprints are preliminary reports that have not undergone peer review.
They should not be considered conclusive, used to inform clinical practice,
or referenced by the media as validated information.

Experimental and Machine Learning Validation of a Modified 2.6 GHz Single-Element Switched-Beam Antenna for 5G sub-6 GHz Applications

Pichaya Chaipanya

pichayac@g.swu.ac.th

Srinakharinwirot University https://orcid.org/0000-0002-6890-9865

Kanyapat Sangchan

Srinakharinwirot University

Korawit Pachuen

Srinakharinwirot University

Nuchanart Santalunai

Rajamangala University of Technology Isan

Samran Santalunai

Suranaree University of Technology

Research Article

Keywords: Switched beam, antenna, 5G communications, 5G sub-6 GHz communications, machine learning, artificial intelligence, simulation time reduction

Posted Date: July 7th, 2026

DOI: https://doi.org/10.21203/rs.3.rs-9146650/v1

License: This work is licensed under a Creative Commons Attribution 4.0 International License.
Read Full License

Experimental and Machine Learning Validation of a Modified 2.6 GHz Single-Element Switched-Beam Antenna for 5G sub-6 GHz Applications

Pichaya Chaipanya[1 *], Kanyapat Sangchan[1], Korawit Pachuen[1], Nuchanart Santalunai[2] and Samran Santalunai[3]

[1]Department of Electrical Engineering, Srinakharinwirot University, Nakhon Nayok, 26120, Thailand
[2]Department of Telecommunication Engineering and Department of Electrical Engineering, Rajamangala University of Technology Isan (RMUTI), Nakhonratchasima, 30000, Thailand
[3]School of Electronic Engineering, Suranaree University of Technology, Nakhonratchasima, 30000, Thailand
[*]Corresponding Author: Pichaya Chaipanya. Email: pichayac@g.swu.ac.th

Abstract: This paper presents the design and implementation of a single-element circular microstrip antenna capable of eight-direction beam switching for fifth generation (5G) sub-6 GHz wireless communication at 2.6 GHz. The antenna operates based on short-circuit control along its edge to steer the main beam toward the desired direction. Electromagnetic simulations were performed using CST Studio Suite, generating 140 datasets for machine learning (ML) training. The input parameters included short-circuit direction, radial distance, number of short-circuit holes, and spacing between holes, while the outputs were the main beam direction (degrees) and reflection coefficient (dB). Four ML algorithms—Gradient Boosting Regression, Lasso Regression, Linear Regression, and Random Forest—were applied to improve design efficiency and reduce simulation time. The Random Forest model achieved the best performance with an R^2 of 1.0 and zero mean error for beam direction prediction, and an R^2 of 0.805 with a mean error of 0.21 for reflection coefficient prediction. The predicted values closely matched CST simulation results, with deviations within ±5 dB. Based on ML predictions, a prototype antenna was fabricated using copper shorting wires, capacitors, and PIN diodes controlled by a microcontroller. Measurements confirmed accurate beam switching in eight directions (0˚, 45˚, 90˚, 135˚, 180˚, 225˚, 270˚, 315˚) at 2.6 GHz. The results demonstrate that the Random Forest algorithm effectively enhances antenna design accuracy, reduces simulation time, and achieves reliable beam-switching performance suitable for compact 5G sub-6 GHz communication systems.

Keywords: Switched beam; antenna; 5G communications; 5G sub-6 GHz communications; machine learning; artificial intelligence; simulation time reduction

1 Introduction

In the era of fifth generation (5G) sub-6 GHz wireless communication [1-3], high-quality signal transmission and rapid response have become essential requirements for modern communication systems. Wireless communication enables reliable long-distance connections and continues to evolve through the development of more compact, cost-effective, and high-performance antennas. Among various antenna types, the microstrip antenna has gained widespread use due to its low profile, light-weight structure, and ease of integration with planar circuits. However, single element microstrip antennas often face limitations in controlling radiation directionality. When the antenna radiates energy in undesired directions, signal interference and degradation may occur. To overcome this issue, switched-beam antenna techniques have been introduced to steer the main beam toward the desired direction while suppressing unwanted side lobes, thereby enhancing communication efficiency and coverage. Several studies have demonstrated the effectiveness of single element switched beam antennas. For example, low-cost, multiband designs for 5G applications [4-5] allow beam switching across multiple frequency bands without the need for complex phased array systems. Other efforts have focused on performance optimization, including reducing backlobe radiation in circular patch antennas to enhance efficiency [6], developing compact antipodal Vivaldi antennas with consistent gain suitable for 5G [7], and using shorting pins in microstrip patches to lower the specific absorption rate (SAR), thereby improving safety and efficiency in mobile applications [8].

Recently, machine learning (ML) has emerged as a powerful tool in antenna design due to its ability to analyze complex parameter relationships and predict antenna performance with high accuracy.

Conventional antenna design often requires extensive electromagnetic (EM) simulations, which are computationally expensive and time-consuming. ML-based modeling can significantly reduce design time by predicting key performance metrics—such as return loss, gain, and beam direction—based on pre-collected simulation data. This approach allows for faster optimization and improves the precision of antenna performance prediction.

Several studies have applied beam-switching and ML techniques to enhance antenna performance. For example, [9] proposed a circular microstrip antenna capable of 360° beam steering using 24 rectangular parasitic strips controlled by PIN diodes, achieving a gain of 1.79 dBi at 3.21–3.54 GHz. In [10], a Yagi–Uda switched-beam antenna array for wireless sensor networks operating at 2.45 GHz was introduced, capable of switching among eight beam directions with a main beam gain above 5.5 dBi. In addition, [11] applied five ML algorithms—Decision Tree, Random Forest, XGBoost Regression, K-Nearest Neighbor (KNN), and Artificial Neural Network (ANN)—to predict the resonant frequency of a single-element antenna, where the KNN model achieved 98% accuracy. Similarly, [12] compared seven ML algorithms to predict antenna resonant frequencies, finding the Decision Tree model to yield the lowest mean squared error (MSE). Furthermore, [13] employed ML to improve the performance of a Quasi-Yagi–Uda antenna using Linear and Gaussian Process Regression, while [14] applied Random Forest to optimize a dual-band F-shaped RFID antenna with an accuracy of 99.96%. Moreover, [15] demonstrated the use of ML algorithms such as KNN and XGBoost to predict the return loss of microstrip antennas, showing that KNN provided superior prediction accuracy.

Although these studies have successfully demonstrated ML-based prediction and switched-beam mechanisms, most existing designs rely on multi-element or diode-controlled structures, which increase complexity, cost, and power consumption. Recent works have also applied ML techniques to predict beam-switching directions in single-element antennas using input features such as the number and position of shorting points [16–19]; however, these studies focused solely on prediction without experimental verification. There remains a need for a compact, single-element switched-beam antenna that can provide efficient beam steering without energy-intensive components, while also integrating ML-based prediction for performance optimization.

To address this gap, this work proposes the design of a 2.6 GHz single-element circular microstrip switched-beam antenna for 5G sub-6 GHz wireless communication applications. The proposed antenna can steer its beam in eight distinct directions while maintaining a compact and energy-efficient structure. ML algorithms are applied to predict two key antenna parameters—the return loss and main beam direction. Four ML algorithms—Gradient Boosting Regression (GBR), Lasso Regression (LR-Lasso), Linear Regression (LR), and Random Forest (RF)—are trained using datasets generated from CST Studio Suite simulations. The predicted results are compared to determine the most effective algorithm for accurate and efficient antenna performance prediction. This study extends our previous work on ML-based switched-beam antenna design by incorporating comprehensive experimental validation and enhanced model evaluation. Unlike the earlier version, which focused primarily on simulation-based analysis, the present work includes fabrication, measurement, and comparative assessment of the proposed antenna. The ML dataset and performance metrics are also refined to verify the practical accuracy of predicted beam directions and return loss. The proposed design aims to contribute to sustainable and energy-efficient wireless infrastructure by combining compact antenna design with intelligent ML-based optimization.

2 Methods

This section describes the methodology used for the design, analysis, and performance prediction of the proposed switched-beam antenna. It is organized into two subsections. The first subsection presents the antenna structure and beam-switching configuration, including the circular microstrip patch design and the placement of short-circuit positions used to control the radiation direction. Key geometric parameters that influence the antenna performance, such as beam direction and return loss, are also discussed. The second subsection introduces the ML models employed to predict antenna performance based on these design parameters. Several regression-based ML algorithms are implemented to model the relationship between

the antenna configuration and its radiation characteristics, enabling efficient performance prediction and reducing the need for extensive full-wave electromagnetic simulations.

2.1 Antenna Design and Beam-switching Configuration

The proposed antenna is designed on an FR-4 substrate with a dielectric constant (ε_r) of 4.4, substrate thickness (h) of 1.6 mm, and ground-plane thickness of 0.03 mm. The radius of the modified circular patch (a) was initially calculated using [20]

$$a = \frac{F}{\left\{1 \times \frac{2h}{\pi \varepsilon_r F}\left[ln\left(\frac{\pi F}{2h}\right) + 1.7726\right]\right\}^{\frac{1}{2}}} \tag{1}$$

where

$$F = \frac{8.791 \times 10^9}{f_r \sqrt{\varepsilon_r}} \tag{2}$$

Then designed in CST Studio Suite, with adjustments made until the antenna operated at the target frequency (f_r) of 2.6 GHz. The final configuration of the antenna is shown in Figure 1, and the corresponding return loss is presented in Figure 2. Beam switching is achieved by introducing short-circuit holes distributed along the edge of the patch. Eight configurations are created by selectively opening and shorting specific positions to redirect the main beam toward eight angular directions.

The modified short-circuit layout differs from conventional uniform patterns by grouping holes into variable-spaced sets, resulting in distinct radiation characteristics across all eight cases. CST Studio Suite simulations confirm that the antenna maintains resonance at 2.6 GHz with return loss below −10 dB for all configurations, while the radiation pattern shape changes slightly according to the switching case. For example, each antenna design uses 56 holes along the edge, with 49 short-circuiting points. The return loss of this antenna remains nearly identical across all eight switching cases, confirming stable operation at 2.6 GHz, as shown in Figure 2. To provide a concise visual comparison, the eight antenna configurations are combined in Figure 3, while the corresponding radiation patterns for all cases are grouped in Figure 4. In Case 1, the activated open-circuit positions at 0°, and the main beam of the radiation pattern points in the same direction, opposite the shorted positions. In Case 2, the open circuits are activated at 45°, producing a main beam at 45°; in Case 3, activation at 90° results in a main beam at 90°; and in Case 4, activation at 135° aligns the main beam with 135°. Similarly, Cases 5 through 8 activate open circuits at 180°, 225°, 270°, and 315°, respectively, with the main beam in each case pointing along the activated open-circuit direction. This demonstrates the antenna's effective beam-switching capability through controlled placement of short and open-circuit points.

2.2 Machine Learning Model for Performance Prediction

In switched-beam microstrip antennas, small geometric variations can strongly influence antenna performance. The patch radius directly affects the resonant frequency, while the short-circuit direction primarily determines the orientation of the main beam. In addition, the radial distance and number of short-circuit holes play a critical role in shaping the radiation behavior; an improper combination of these parameters may fail to produce the desired beam direction or result in non-directional patterns. Although the main beam direction in an ideal switched-beam antenna is geometrically associated with the open-circuit

location, practical beam steering behavior is not solely determined by this parameter. In the proposed antenna, the beam direction and radiation quality are jointly influenced by multiple interacting factors. For example, an insufficient number of short-circuit holes or improper spacing can prevent effective beam switching or introduce high sidelobe levels, while variations in radial distance can shift the resonant frequency, leading to degraded return loss at the target frequency of 2.6 GHz. Moreover, even when the same short-circuit direction is applied, the main beam may deviate from the ideal direction (e.g., a measured offset of several degrees), indicating that the beam response is not strictly deterministic. These coupled and nonlinear effects make rule-based or purely geometric prediction insufficient, motivating the use of machine learning to capture complex relationships among design parameters and to reliably predict both beam direction and return loss under practical conditions.

A total of 150 simulated data samples were generated using CST Studio Suite. Among these, 140 samples were used for machine learning model development and were divided into a training set of 112 samples (80%) and a test set of 28 samples (20%). In addition, 10 independent simulation cases, not included in the training or test datasets, were generated and used solely to evaluate the prediction accuracy of the models. The relatively limited dataset size is a consequence of the high computational cost of full-wave electromagnetic simulations and reflects the proof-of-concept nature of this study rather than an attempt to achieve full statistical generalization. Each dataset includes four input parameters: short-circuit direction (group number) (In1), radial distance from patch center to short position (In2), number of short-circuit holes (In3), and spacing between shorted groups (In4). The target outputs are: main beam direction (degrees), and return loss (dB).

Four regression-based ML algorithms—GBR, LR-Lasso, LR, and RF—were implemented using Python. The models were trained using the training dataset and evaluated on the test dataset. The key hyperparameters used for each algorithm are summarized in Table 1. In the RF model, the number of estimators was set to 100 with a random state of 42 to ensure reproducibility. The LR model was implemented with the intercept term enabled (fit_intercept = True). For the GBR model, the learning rate was set to 0.1 and the number of estimators was set to 75 to balance model accuracy and complexity. The LR-Lasso model used a regularization parameter (alpha) of 0.01, which provided the best performance for the given dataset. Although k-fold cross-validation is commonly used to improve model generalization, it was not applied in this study due to the computational cost associated with repeated electromagnetic simulations. Instead, a fixed training–test split was adopted. In addition, an independent set of simulation cases, excluded from both the training and test datasets, was used to further evaluate the robustness and prediction capability of the models. The prediction performance was evaluated using the coefficient of determination (R^2) and mean absolute error (MAE), defined as [21]

$$MAE = \frac{1}{N}\sum_{i=1}^{N}\left|y_i - y_i\right| \tag{3}$$

$$R^2 = 1 - \left(\sum_{i=1}^{N}\left(y_i - y_i\right)^2 \Big/ \sum_{i=1}^{N}\left(y_i - \bar{y}\right)^2\right) \tag{4}$$

where N is the total number of samples, y_i and y_i represent the simulated and predicted values, respectively, and $\bar{y}$ denotes the mean of the simulated values. The results are summarized in Table 2 for main beam direction prediction and Table 3 for return loss prediction.

Table 1: Hyperparameters of the ML models.

Algorithm	Hyperparameters	Values
RF	n_estimators	100
	random_state	42

LR	fit_intercept	True
GBR	learning_rate	0.1
	n_estimators	75
LR-Lasso	alpha	0.01

Table 2: Main beam prediction.

inputs				outputs				
In1	**In2**	**In3**	**In4**	**CST**	**GBR**	**LR-Lasso**	**LR**	**RF**
1	51.0	77	4.0	0	0.1	0	0	0
1	49.0	63	4.0	0	0.1	0	0	0
2	48.0	49	6.0	45	43.04	45	45	45
3	51.0	35	6.0	90	90	90	90	90
4	51.0	35	6.0	135	135	135	135	135
5	48.5	49	5.0	180	180	180	180	180
6	49.5	63	4.0	225	225	225	225	225
6	49.5	35	5.0	225	225	225	225	225
7	50.0	49	4.5	270	272.3	270	270	270
8	49.5	63	4.5	315	314.89	315	315	315
R^2					1	1	1	1
MAE					0.447	0	0	0

Table 3: Return loss prediction.

inputs				outputs				
In1	**In2**	**In3**	**In4**	**CST**	**GBR**	**LR-Lasso**	**LR**	**RF**
1	51.0	77	4.0	13.23	14.09	12.06	12.08	13.94
1	49.0	63	4.0	13.52	13.65	12.91	13.33	12.82
2	48.0	49	6.0	13.97	13.55	14.02	15.61	14.17
3	51.0	35	6.0	10.06	16.48	15.23	15.18	12.08
4	51.0	35	6.0	14.26	13.28	11.91	11.95	13.04
5	48.5	49	5.0	13.03	14.10	14.52	14.40	13.72
6	49.5	63	4.0	13.40	19.20	15.46	14.96	13.23
6	49.5	35	5.0	9.49	13.92	13.15	13.18	13.35
7	50.0	49	4.5	11.96	13.81	12.79	12.63	12.59
8	49.5	63	4.5	13.42	11.93	13.63	13.21	12.83
R^2					0.898	0.544	0.800	0.805
MAE					0.520	0.271	0.239	0.210

For main beam direction prediction, LR, LR-Lasso, and RF achieved perfect accuracy ($R^2 = 1$, MAE = 0), reflecting the strong linear relationship between beam direction and short-circuit position. GBR also

performed well but exhibited a slightly higher MAE due to its sensitivity to nonlinear variations. These results indicate that beam direction prediction is largely deterministic when the short-circuit geometry is properly defined.

In contrast, return loss predictions exhibited more complex and nonlinear behavior. Among the evaluated models, the RF algorithm achieved the lowest MAE of 0.21 with an R^2 value of 0.805, demonstrating reliable performance in modeling nonlinear electromagnetic responses. The LR model also produced a relatively high R^2 of 0.800 with an MAE of 0.239, while LR-Lasso achieved an R^2 of 0.544 and an MAE of 0.271. Although the GBR model achieved the highest R^2 value of 0.898, it produced the largest prediction error with an MAE of 0.520 among the evaluated models. Therefore, considering both accuracy and prediction error, the RF model provides the most balanced performance for return loss prediction. Overall, RF was the most reliable algorithm, accurately predicting main beam directions and achieving the lowest average error for return loss. These results suggest that RF is well suited for ML-assisted antenna analysis under limited-data conditions, providing robust performance for both linear and nonlinear characteristics.

3 Results and Discussion Section

This section presents the fabrication and performance evaluation of a single-element antenna capable of switching its main beam in eight directions. Antenna parameters were derived from a ML–predicted dataset (Section 2) and used to construct a physical prototype. Performance was assessed based on radiation patterns and return loss, and results were compared with CST Studio Suite simulations for validation.

The fabricated antenna features a substrate thickness of 1.6 mm, with the conductive patch and ground plane each 0.03 mm thick. The square patch measures 150 × 150 mm^2, with a dielectric constant of 4.4. Using the sixth dataset input (Table 2 and Table 3), a circular patch of 48.5 mm radius was implemented. Fifty-six holes were drilled along the perimeter with 5 mm spacing; seven were used for active switching, while the remaining were short-circuited with copper wires. Diodes and capacitors were soldered along the circle to control beam switching. The eight beam-switching cases were implemented using the same single-element antenna shown in Figure 5. For each case, a specific set of seven holes along the patch perimeter was opened, while the remaining 49 holes were short-circuited. By selectively biasing the corresponding diodes, the antenna could switch its main beam sequentially to 0˚ (top), 45˚ (top-right), 90˚ (right), 135˚ (bottom-right), 180˚ (bottom), 225˚ (bottom-left), 270˚ (left), and 315˚ (top-left) without the need for multiple elements, enabling efficient operation using a single patch.

All eight beam-switching cases were tested at 2.6 GHz, with a microcontroller controlling the diode bias to open or short-circuit the appropriate holes. The measured return loss values ranged from 12.26 dB to 15.34 dB across all beam-switching cases, with an average value of 14.25 dB. Figure 6 presents the measured return loss for Case 1 as a representative example, demonstrating stable impedance matching behavior of the antenna. Radiation pattern measurements in Fig. 7 show that the main beam of the fabricated antenna generally aligns with the intended open-circuit direction, demonstrating good overall agreement with CST Studio Suite simulations. Although most cases show close agreement between simulation and measurement, several cases exhibit noticeable beam shifts. Specifically, Case 4 shifts from 135˚ (simulated) to 165˚ (measured), Case 5 from 180˚ to 200˚, and Case 8 from 315˚ to 300˚. The maximum observed beam deviation is 30˚. These deviations are mainly attributed to practical implementation effects that were not fully included in the CST model, such as the parasitic impedance of PIN diodes, biasing circuits, solder joints, and connecting wires. These elements can alter the current distribution along the antenna structure and slightly modify the resulting radiation pattern. It should be noted that the proposed antenna operates as a switched-beam antenna designed to provide directional coverage across discrete angular sectors rather than precise beam pointing. Despite the observed deviations, the measured radiation patterns clearly demonstrate beam switching toward the intended directional regions, confirming the practical feasibility of the proposed antenna and supporting the effectiveness of the ML-assisted design approach.

The predicted return loss ranged from 13.7 to 14.7 dB, closely matching both simulations and measurements as shown in Table 4 and Table 5. These results confirm that the antenna achieves reliable

beam steering and consistent reflection performance as designed.

Table 4: Simulation, ML, and measurement results of main beam direction

In1	CST	GBR	LR-Lasso	LR	RF	Measurement
1	0	2.83	0	0	0	0
2	45	45.003	45	45	45	45
3	90	90.00	90	90	90	90
4	135	137.41	135	135	135	165
5	180	180	180	180	180	200
6	225	225	225	225	225	225
7	270	269.93	270	270	270	270
8	315	314.14	315	315	315	300

Table 5: Simulation, ML, and measurement results of corresponding return loss

In1	CST	GBR	LR-Lasso	LR	RF	Measurement
1	14.16	14.13	14.47	14.32	14.63	15.17
2	14.11	14.12	14.49	14.36	14.58	15.34
3	13.85	13.69	14.50	14.40	14.52	14.49
4	14.11	14.08	14.44	14.46	14.51	12.26
5	13.85	14.10	14.47	14.40	14.52	14.22
6	13.89	14.07	14.47	14.34	14.69	14.83
7	13.85	14.09	14.55	14.28	14.54	14.54
8	13.89	13.74	14.59	14.23	14.55	13.16

These results demonstrate that the antenna performs reliably according to design specifications. Moreover, the study confirms that ML can effectively assist in antenna design by predicting and refining parameters, thereby enhancing design accuracy and overall performance.

4 Conclusion

This work presented the design and fabrication of a single-element antenna capable of switching its main beam across eight directions at 2.6 GHz for 5G sub-6 GHz wireless communication. The beam-switching mechanism relies on selectively short-circuiting holes along the patch perimeter. A total of 112 simulated datasets generated from CST Studio Suite were used to ML models. Four regression algorithms—GBR, LR-Lasso, LR, and RF—were applied to predict the main beam direction and return loss. Among the tested models, RF achieved the best performance, obtaining an R^2 of 1 and MAE of 0 for beam direction prediction, and an R^2 of 0.805 with MAE of 0.21 for return loss prediction. These results showed strong agreement with CST simulations. Using the predicted parameters, a prototype antenna was fabricated, with copper wires short-circuited on the front patch and diodes and capacitors soldered on the back, controlled via a microcontroller for beam switching. Experimental results verified that the antenna successfully steers its main beam toward the intended directions of 0˚, 45˚, 90˚, 135˚, 180˚, 225˚, 270˚, and 315˚. The measured radiation patterns generally agree with CST simulations and ML predictions, with minor deviations attributed to practical implementation effects. These findings demonstrate that ML, particularly the RF model, can effectively assist antenna design by reducing simulation effort while maintaining strong agreement with experimental results.

For future work, prediction performance could be further improved by exploring more advanced ML

approaches such as neural networks or deep learning models. In addition, expanding the dataset beyond 112 samples through additional CST simulations may improve prediction accuracy, particularly for parameters with more complex behavior such as return loss.

Abbreviations

5G	Fifth-Generation
ML	Machine Learning
SAR	Specific Absorption Rate
EM	Electromagnetic
KNN	K-Nearest Neighbor
ANN	Artificial Neural Network
MSE	Mean Squared Error
GBR	Gradient Boosting Regression
LR-Lasso	Lasso Regression
LR	Linear Regression
RF	Random Forest
R^2	R-squared
MAE	Mean Absolute Error

Declarations

Availability of data and materials

The datasets generated and/or analyzed during the current study are available from the authors on reasonable request.

Competing interests

The authors declare that they have no competing interests.

Funding

This work was supported by Srinakharinwirot University (SWU) and Faculty of Engineering, SWU, Thailand through the research grant No. 494/2567.

Authors' contributions

PC conceived the study, supervised the research, and designed the antenna. KS developed the machine learning models, collected simulation data, and fabricated the antenna prototype. KP conceived the antenna design and participated in the antenna fabrication. NS performed simulations and data analysis. SS prepared and adjusted the antenna layout prior to fabrication. All authors contributed to drafting the manuscript, and all read and approved the final version.

Acknowledgements

The authors would like to acknowledge the financial support from Srinakharinwirot University (SWU), Thailand through the research grant No. 494/2567 and the Faculty of Engineering, SWU, Thailand. The authors also gratefully acknowledge institutional support from Srinakharinwirot University, Rajamangala University of Technology Isan (RMUTI), and Suranaree University of Technology, Thailand.

References

[1] H. Yuhong, Challenges and opportunities of sub-6 GHz integrated sensing and communications for 5G-advanced and beyond. Chinese Journal of Electronics **33**(2), 323–325 (2024)

[2] Communications looking back at 5G to build future 6G in ITU-R, https://research.samsung.com/blog/Looking-back-at-5G-to-build-future-6G-in-ITU-R, [accessed 18.10.2025]

[3] 5 key differences between mmWave and sub-6GHz, https://rimedolabs.com/blog/5-key-differences-between-mmwave-and-sub-6ghz/, [accessed 18.10.2025]

[4] Z. Zahar and M. F. Bin Ain, Backlobe reduction of air substrate circular patch antenna for 5G applications. in Proceedings: 11th International Conference on Robotics, Vision, Signal Processing and Power Applications. 948–954, (2022)

[5] D. Wang, X. Wei, J. Zhang, Y. Shu and D. Yang, Back lobe reduction of patch antenna by using high-impedance surface (Invited). in Proceedings: IET International Radar Conference 2015. 1–4 (2015)

[6] M. T. Ali, T. A. Rahman, M. R. Kamarudin, R. Sauleau, M. N. M. Tan and M. F. Jamlos, A reconfigurable planar antenna array (RPAA) with back lobe reduction. in Proceedings: 2010 International Workshop on Antenna Technology (iWAT). 1-4 (2010)

[7] R. Liu, K. Ma, N. Yan, Y. Wang and Y. Wu, An FR4-based miniaturized high-efficiency double-sided SISL longitudinal slot antenna array for 5G Millimeter-Wave applications. IEEE Transactions on Antennas and Propagation **72**(7), 6099-6104 (2024)

[8] U. Singh and R. Mishra, A dual-band high-gain substrate integrated waveguide slot antenna for 5G application. Progress In Electromagnetics Research C. 119. 191-200 (2022)

[9] N. D. Hoang, K. Monai and T. L. Dinh, A design of switched-beam Yagi-Uda antenna for wireless sensor networks. in Proceedings: 2016 IEEE Conference on Advanced Technologies for Communications (ATC). 393-396 (2016)

[10] D. Sourave, R. T. Husnur and A. R. Muhammad, Design of a microstrip antenna having 360° beam steering capability in azimuth plane. in Proceedings: 2022 IEEE Conference on Electrical and Computer Engineering (ICECE). 136-139 (2022)

[11] P. Ranjan, A. Maurya, H. Gupta, S. Yadav and A. Sharma, Ultrawideband CPW fed band-notched monopole antenna optimization using machine learning. Progress In Elec-tromagnetics Research M. 108. 27-38 (2022)

[12] M. A. Haque, N. Sarker, N. S. Sawaran Singh, M. A. Rahman, M. N. Hasan, M. Islam, M. A. Zakariya, L. C. Paul, A. H. Sharker, G. E. M. Abro, M. Hannan and R. Pk, Dual band antenna design and prediction of resonance frequency using machine learning approaches. Applied Sciences. **12**(10505). 1-18 (2022)

[13] M. A. Haque, M. A. Rahman, S. S. Al-Bawri, Z. Yusof, A. H. Sharker, W. M. Abdulkawi, D. Saha, L. C. Paul and M. A. Zakariya, Machine learning-based technique for gain and resonance prediction of mid band 5G Yagi antenna. Scientifc Reports. **13**(12590). 1-22 (2023)

[14] Y. Nuray and N. Akcam, Designing of dual band F-shaped RFID antenna using machine learning techniques. Journal of Artificial Intelligence and Data Science (JAIDA). **2**(2). 69-75 (2022)

[15] R. Jain, P. Ranjan, P. K. Singhal and V. V. Thakare, Estimation of S11 values of patch antenna using various machine learning models. in Proceedings: 2022 IEEE Conference on Interdisciplinary Approaches in Technology and Management for Social Innovation (IATMSI). 1-4 (2022)

[16] W. Noimi and P. Chaipanya, Wide-band circular slot antenna beam switching directions using machine learning algorithms. in Proceedings: IEEE Asia Pacific Conference on Circuits and Systems (APCCAS). 484-488 (2024)

[17] O. Nikornpon and P. Chaipanya, Predicting beam switching directions in ultrawideband spiral antennas using machine learning algorithms. in Proceedings: IEEE Asia Pacific Conference on Circuits and Systems (APCCAS). 479-483 (2024)

[18] K. Sangchan and P. Chaipanya, Enhancement of beam switching in single element antenna using machine learning. in Proceedings: SICE International Symposium on Control Systems (SICE ISCS). 76-80 (2025)

[19] P. Chaipanya, W. Noimi, S. Wintachai, S. Wisetlertmongkol, N. Santalunai and S. Santalunai, A Two-Stage Machine Learning Framework for Predicting and Validating the Structural and Beam Characteristics of a Wideband Switched-Beam Antenna. IEEE Access. **14**(2026). 27865 – 27876 (2026)

[20] C.A. Balanis, Antenna Theory: Analysis and Design, 3rd ed. John Wiley & Sons, (2015)

[21] D. Chicco, MJ. Warrens, G. Jurman, The coefficient of determination R-squared is more informative than SMAPE, MAE, MAPE, MSE and RMSE in regression analysis evaluation. PeerJ Computer Science **7**:e623. (2021)

Figures, Figure Title and Legend Section

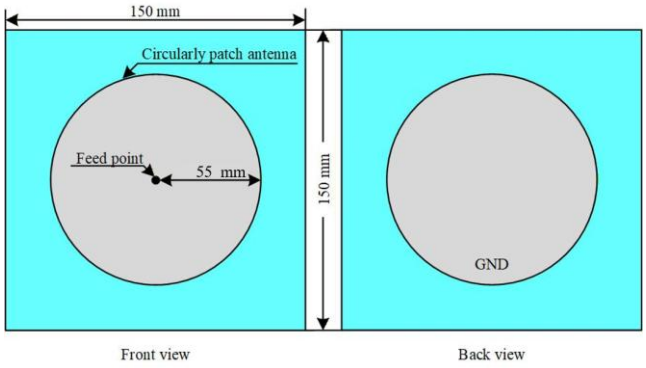


Figure 1: Configuration of the antenna without short circuit.

Detailed: Final configuration of the proposed single-element switched-beam antenna.

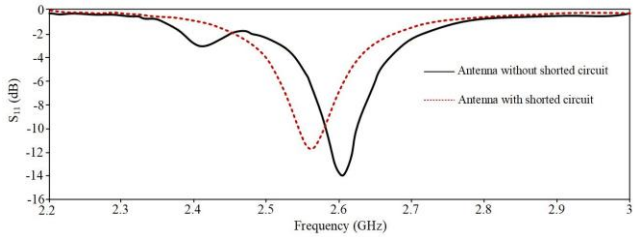


Figure 2: The corresponding return loss of the antenna with and without short circuit.

Detailed: Simulated return loss of the antenna operating at 2.6 GHz.

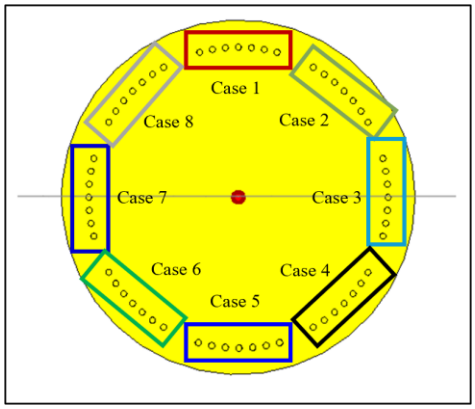


Figure 3: Configuration of the antenna with short circuit.

Detailed: Eight antenna configurations obtained by changing the short-circuit positions along the patch edge.

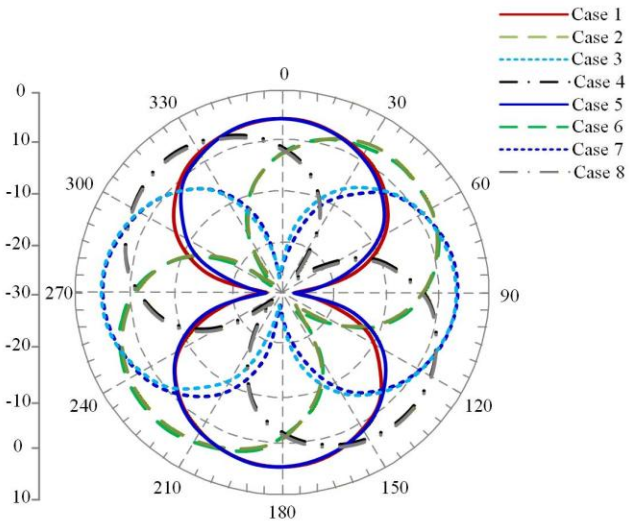


Figure 4: Radiation pattern of the antenna with short circuit.

Detailed: Simulated radiation patterns corresponding to the eight switching configurations.

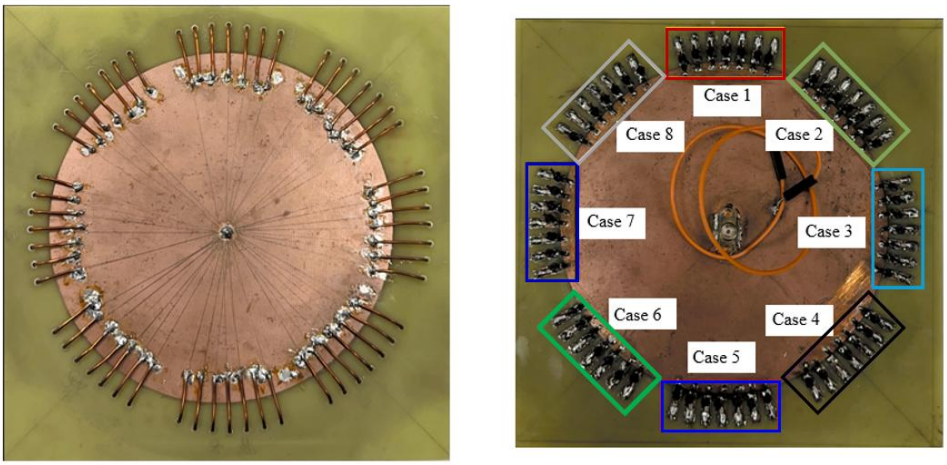


Figure 5: Configuration of the experiment antenna with diodes and capacitors.

Detailed: Implementation of the eight beam-switching cases using the same single-element antenna structure.

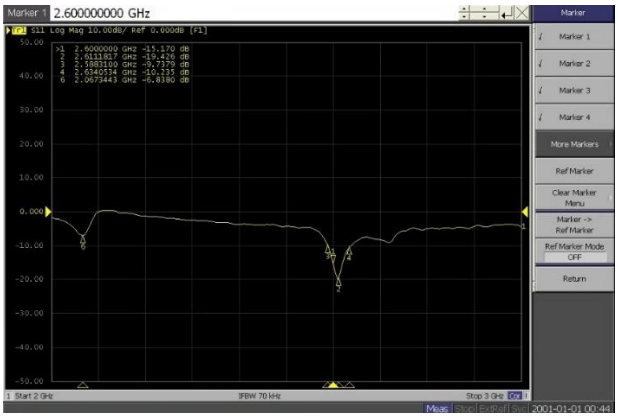


Figure 6: The corresponding return loss of the experiment antenna with short circuit.

Detailed: Measured return loss for Case 1 shown as a representative example of the fabricated antenna performance.

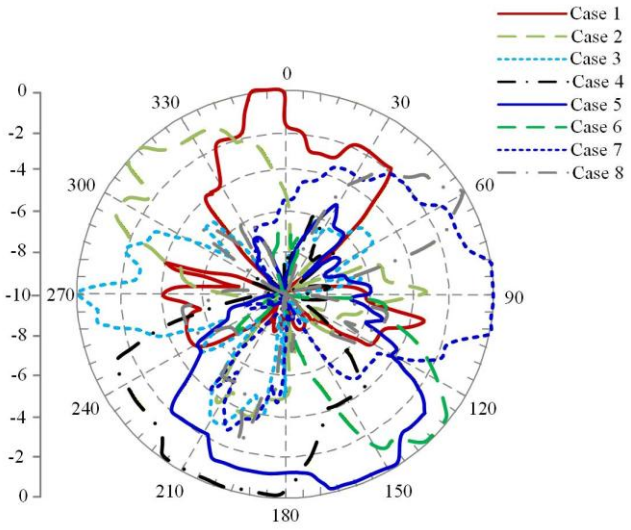


Figure 7: Radiation pattern of the experiment antenna.

Detailed: Measured radiation patterns illustrating the main beam directions of the fabricated antenna.